

# Dynamics of gas bubbles in viscoelastic fluids. I. Linear viscoelasticity

John S. Allen, and Ronald A. Roy

Citation: [The Journal of the Acoustical Society of America](#) **107**, 3167 (2000); doi: 10.1121/1.429344

View online: <https://doi.org/10.1121/1.429344>

View Table of Contents: <https://asa.scitation.org/toc/jas/107/6>

Published by the [Acoustical Society of America](#)

---

## ARTICLES YOU MAY BE INTERESTED IN

[Dynamics of gas bubbles in viscoelastic fluids. II. Nonlinear viscoelasticity](#)

[The Journal of the Acoustical Society of America](#) **108**, 1640 (2000); <https://doi.org/10.1121/1.1289361>

[A model for the dynamics of gas bubbles in soft tissue](#)

[The Journal of the Acoustical Society of America](#) **118**, 3595 (2005); <https://doi.org/10.1121/1.2118307>

[Numerical modeling of bubble dynamics in viscoelastic media with relaxation](#)

[Physics of Fluids](#) **27**, 063103 (2015); <https://doi.org/10.1063/1.4922598>

[Nonlinear oscillations following the Rayleigh collapse of a gas bubble in a linear viscoelastic \(tissue-like\) medium](#)

[Physics of Fluids](#) **25**, 083101 (2013); <https://doi.org/10.1063/1.4817673>

[Linear oscillation of gas bubbles in a viscoelastic material under ultrasound irradiation](#)

[Physics of Fluids](#) **27**, 113103 (2015); <https://doi.org/10.1063/1.4935875>

[A generalization of the Rayleigh–Plesset equation of bubble dynamics](#)

[The Physics of Fluids](#) **25**, 409 (1982); <https://doi.org/10.1063/1.863775>

---

# Dynamics of gas bubbles in viscoelastic fluids. I. Linear viscoelasticity

John S. Allen

*Department of Biomedical Engineering, One Shields Avenue, University of California, Davis, Davis, California 95616*

Ronald A. Roy

*Department of Aerospace and Mechanical Engineering, Boston University, 110 Cummington Street, Boston, Massachusetts 02215*

(Received 17 May 1999; accepted for publication 13 March 2000)

The nonlinear oscillations of spherical gas bubbles in linear viscoelastic fluids are studied. A novel approach is implemented to derive a governing system of nonlinear ordinary differential equations. The linear Maxwell and Jeffreys models are chosen as the fluid constitutive equations. An advantage of this new formulation is that, when compared with previous approaches, it facilitates perturbation methods and numerical investigations. Analytical solutions are obtained using a multiple scale perturbation method and compared with the Newtonian results for various Deborah numbers. Numerical analysis of the full equations supports the perturbation analysis, and further reveals significant differences between the viscoelastic and Newtonian cases. Differences in the oscillation phase and harmonic structure characterize some of the viscoelastic effects. Subharmonic excitations at particular fluid parameters lead to a discrete group modulation of the radial excursions; this appears to be a unique, previously undiscovered phenomenon. Implications for medical ultrasound applications are discussed in light of these current findings. © 2000 Acoustical Society of America. [S0001-4966(00)04606-3]

PACS numbers: 43.35.Wa, 43.25.Yw, 43.80.Gx [HEB]

## LIST OF SYMBOLS

$\lambda_1$	relaxation time	$\bar{a} = p_a/p_0$	ratio of pressure amplitudes
$\lambda_2$	retardation time	$De = \lambda_1/R_0\sqrt{\rho/p_{go}}$	Deborah number (perturbation analysis)
$\dot{\varsigma}$	rate of strain or deformation tensor	$\lambda = \lambda_2/\lambda_1$	ratio of time fluid time constants
$\eta_0$	zero shear-rate viscosity	$x$	relative amplitude in perturbation analysis
$\kappa$	polytropic exponent	$a$	real part of amplitude in perturbation analysis
$S(R,t) = \int_R^\infty (\tau_{rr}(r,t) dr/r)$	spatial integral over radial stress	$\omega_0^2 = 3\kappa - w$	detuning parameter (perturbation analysis)
$\bar{r} = r/R_0$	nondimensional radial coordinate	$\sigma$	nondimensional time (numerical analysis)
$\bar{R} = R/R_0$	nondimensional bubble radius	$\bar{t} = \omega t$	Deborah number (numerical analysis)
$\bar{t} = t/R_0\sqrt{\rho/p_{go}}$	nondimensional time (perturbation analysis)	$De = \lambda_1\omega$	Reynolds number (numerical analysis)
$\bar{\tau} = \tau/\eta_0 R_0\sqrt{\rho/p_{go}}$	nondimensional radial stress	$Re = \rho\omega R_0^2/\eta_0$	
$w = 2\hat{\sigma}/p_{go}R_0$	nondimensional Laplace pressure		
$\Omega = R_0\sqrt{\rho/p_{go}}\omega$	ratio of forcing frequencies		
$Re = \eta_0/(p_{go}\rho)^{1/2}R_0$	Reynolds number (perturbation analysis)		

## INTRODUCTION

The nonlinear oscillations of an isolated, acoustically forced gas bubble have been the subject of extensive research.<sup>1,2</sup> Most of these studies have concentrated on the behavior of gas bubbles in Newtonian fluids. However, there is a growing interest in the nature of gas bubble oscillations in non-Newtonian fluids. In part, this interest has been motivated by the increasingly important role of cavitation

and associated bubble dynamics in medical ultrasound applications,<sup>3,4</sup> where biological fluids and tissues often exhibit non-Newtonian behavior.<sup>5,6</sup> Unfortunately, a complete and comprehensive study of the various rheological properties of tissue is still far from complete. Nevertheless, bubbles are proving to be valuable tools for medical diagnosis as evidenced by the emergence of ultrasound contrast agents, which usually take the form of microbubbles introduced into

a patient's bloodstream to increase ultrasound scattering for enhanced image contrast.<sup>7</sup> Another biomedical area of growing importance is the monitoring and assessment of possible cavitation bioeffects from medical ultrasound;<sup>8</sup> however, there remains some debate as to which modalities and parameter ranges of medical ultrasound might produce cavitation bioeffects. Within this context, one of the limitations of current research efforts is the lack of a model for bubble dynamics that properly accounts for tissue rheology. Previous theoretical efforts at determining cavitation bioeffect criteria have been based on an understanding of Newtonian bubble dynamics,<sup>8</sup> a fact that has complicated the detailed, quantitative comparison of theoretical predictions and *in vivo* studies. Thus, there exists a need to account for the impact of non-Newtonian rheology on the dynamics of bubbles in biomedical systems.

The scope of this problem, however, extends well beyond the aforementioned biomedical applications. Research topics as diverse as the acoustic scattering from oceanic microbubble-cloud targets, cavitation erosion suppression studies, cavitation dynamics in food processing, decompression sickness and sonochemistry all involve bubbles in non-Newtonian fluids to one extent or another. The study of bubbles in non-Newtonian polymeric solutions is particularly germane to polymer processing and other industrial applications. Bubble behavior in polymeric solutions has been modeled in many previous studies using empirical shear-thinning constitutive relationships.<sup>9</sup> This approach has been employed for acoustically forced bubble oscillations. In these studies, the only non-Newtonian effect considered is shear thinning (viscosity modeled as a decreasing function of the shear stress). A less understood, and perhaps more profound non-Newtonian effect is viscoelasticity, a feature that is particularly relevant to many biomaterials.<sup>5,6</sup> From the physical point of view, dilation accompanying spherical bubble oscillations "stretches" the fluid, a scenario in which viscoelastic effects are important. Hence viscoelasticity, and its effect on spherical bubble dynamics, is the focus of this paper.

In 1970, Fogler and Goddard published a groundbreaking study of the free oscillations of a spherical bubble in a viscoelastic fluid.<sup>10</sup> For simplicity, they modeled the bubble as an empty void and used the linear Maxwell model as the constitutive equation for the surrounding fluid. They mathematically combined this constitutive equation with a Rayleigh-Plesset bubble dynamics formulation<sup>10</sup> in deriving an integro-differential equation for the radial dynamics. This equation was examined in certain asymptotic limits and solved numerically for a few cases. Their results suggested that for certain parameter ranges, the elasticity of the fluid retards the bubble collapse. However, numerical difficulties limited their integration to only a few cycles of bubble oscillation. Moreover, their choice of a void with no internal gas pressure constrains the physical interpretation of their results. Following the work of Fogler and Goddard, Tanasawa and Yang, and later Ting, studied a freely oscillating bubble using a three-constant Oldroyd constitutive equation.<sup>11,12</sup> Numerical difficulties in solving the resulting integro-differential equation also limited the scope of these

investigations. More recently, Kim undertook a study of the free oscillations of a non-Newtonian bubble with an objective form of the Maxwell model, solving the  $r$  and  $\theta$  components of the continuity, momentum and constitutive equations simultaneously using a finite-element method.<sup>13</sup> Kim's effort proved to be too computationally intensive to admit a comprehensive study of bubble behavior for a wide range of parameter values.

The investigation of acoustically forced bubble oscillations has received less attention. Shima and co-workers examined an acoustically forced bubble with the three-constant Oldroyd model<sup>14</sup> for the fluid. Their study provides some intriguing results; however, it was a pioneering study and thus left many fundamental questions unanswered.

One advantage of using the "objective" constitutive equations as opposed to a linear viscoelastic formulation is that the former is intrinsically valid for large deformations of the fluid. The term "objective" refers to the property of being invariant under changes in reference frame; observers subject to relative motion between each other see the same stress on a body. Furthermore, it has been demonstrated that some of these equations originate from molecular level considerations as opposed to empirical, macroscopic assumptions.<sup>15</sup> Conversely, linear viscoelastic equations originate mostly from empirical arguments. Nevertheless, even for linear viscoelastic fluids, bubble dynamics is poorly understood and, in particular, the behavior of acoustically forced bubbles remains relatively unexplored. This is due, in part, to the numerical difficulties associated with solving Fogler and Goddard's radial viscoelastic bubble equation. (More recently, researchers have attempted to compare their results from a more complicated constitutive equation with this original work.<sup>13</sup>) A more comprehensive study of bubble dynamics in linear viscoelastic fluids is justified, particularly as a prelude to tackling the complications associated with the adoption of objective constitutive relationships.

Thus this study will demonstrate that the linear viscoelastic bubble dynamics equations can be obtained using a novel approach offering several advantages over previous formulations. The governing equations are a system of nonlinear, ordinary differential equations. This allows for a robust numerical study and direct implementation of a standard perturbation analysis. These two methods of solution complement each other, yielding new physical insight into the bubble dynamics. The perturbation analysis facilitates a qualitative comparison with some of the previous results on resonance forcing behavior. The numerical investigations reveal intriguing, previously unreported phenomena.

Moreover, it is important to keep in mind the physical assumptions underpinning the linear viscoelastic constitutive equations. There are associated constraints on the amount of physically realizable radial deformation (i.e., growth and rebound) the bubble can assume, and hence on the overall magnitude of acoustic forcing. The perturbation method employed is similar to that previously used for the Newtonian case. This method is implemented for small-amplitude oscillations about the equilibrium radius; thus, the linear viscoelastic excursion limitations are satisfied. Nonlinear viscoelastic damping terms come in at a higher order and are

not considered in the analyses. Also, in the linear viscoelastic case the stress tensor is traceless, which simplifies the analysis since we need only consider the radial component of the stress tensor.

## I. GOVERNING EQUATIONS

The Rayleigh-Plesset equation for a gas bubble can be written in a general form, given in Eq. (1), which includes the stress tensor of the liquid.<sup>10</sup> This equation describes the motion of a spherically symmetric bubble of radius  $R(t)$  in an incompressible fluid of density  $\rho$  subject to a static surface tension  $\hat{\sigma}$ , an internal gas pressure  $p_i$ , and an ambient pressure  $p_\infty$ . For the linear viscoelastic (traceless) case, we need only consider the radial stress component,

$$R\ddot{R} + \frac{3}{2}\dot{R}^2 = \frac{1}{\rho_0} \left[ p_i - p_\infty - \frac{2\hat{\sigma}}{R} - 3 \int_R^\infty \frac{\tau_{rr} dr}{r} \right]. \quad (1)$$

This equation is coupled to a constitutive equation for the fluid which in turn relates the radial stress tensor,  $\tau_{rr}$ , to the spatial deformations in the fluid.

The linear Jeffreys model is chosen as the constitutive equation for this study.<sup>15</sup> It has been used as a starting point for more complicated models and reduces to the linear Maxwell model used by Fogler and Goddard in the case that the retardation time as defined below goes to zero.<sup>15</sup> The Jeffreys model can be expressed as

$$\tau_{rr} + \lambda_1 \frac{\partial \tau_{rr}}{\partial t} = -2\eta_0 \left( \dot{\epsilon} + \lambda_2 \frac{\partial \dot{\epsilon}}{\partial t} \right), \quad (2a)$$

$$\dot{\epsilon} = \frac{\partial u}{\partial r} = -\frac{2\dot{R}R^2}{r^3}; \quad u = \frac{\dot{R}R^2}{r^2}, \quad (2b)$$

where  $\lambda_1$  is the relaxation time,  $\lambda_2$  is the retardation time,  $\dot{\epsilon}$  is the rate of strain or deformation tensor, and  $\eta_0$  is the zero shear-rate viscosity. The relaxation time refers to the time it takes the stress to fall to  $1/e$  of its original equilibrium value and the retardation time is the time it takes the strain to fall to  $1/e$  of its equilibrium value after the removal of stress. The radial component of the deformation tensor corresponding to Eq. (2a) may be expressed as  $\partial u / \partial r$ , where  $u$  is radial velocity in the liquid for the bubble.<sup>9-14</sup> The radial stress, which results from the solution to (2), is coupled to Eq. (1) through a spatial integral over the surrounding fluid. Previous approaches such as that taken by Fogler and Goddard first solved the constitutive equation for the stress tensor Eq. (2) in terms of time and then substituted the resulting expression into the integral in Eq. (1).<sup>10-12</sup> Integration was subsequently performed in terms of the spatial variable. In this new approach, the stress tensor is first solved in terms of the spatial variables. We substitute from Eq. (2b) the deformation tensor in terms of the radial fluid velocity. Equation (2) is first divided by  $r$  and then integrated from the bubble wall to infinity,

$$\begin{aligned} \int_R^\infty \frac{\tau_{rr}(r,t) dr}{r} + \lambda_1 \int_R^\infty \frac{\partial}{\partial t} \left( \frac{\tau_{rr}(r,t)}{r} \right) dr \\ = 4\eta_0 \left[ \int_R^\infty \frac{\dot{R}R^2 dr}{r^4} + \lambda_2 \int_R^\infty \frac{2R\dot{R}^2 + R^2\ddot{R} dr}{r^4} \right]. \end{aligned} \quad (3)$$

The Leibnitz Rule can be used to simplify the second term on the left-hand side of Eq. (3),

$$\begin{aligned} \int_R^\infty \frac{\partial}{\partial t} \left( \frac{\tau_{rr}(r,t)}{r} \right) dr = \frac{d}{dt} \int_R^\infty \frac{\tau_{rr}(r,t) dr}{r} \\ + \frac{dR}{dt} \frac{\tau_{rr}(R(t))}{R}. \end{aligned} \quad (4)$$

Equation (4) is substituted into Eq. (3), and the two terms on the right-hand side of Eq. (3) are integrated out analytically, yielding the following equation:

$$\begin{aligned} \int_R^\infty \frac{\tau_{rr}(r,t) dr}{r} + \lambda_1 \left( \frac{d}{dt} \int_R^\infty \frac{\tau_{rr}(r,t) dr}{r} + \dot{R} \frac{\tau_{rr}(R(t))}{R} \right) \\ = \frac{4}{3} \eta_0 \left( \frac{\dot{R}}{R} + \lambda_2 \left( \frac{2\dot{R}^2 + R\ddot{R}}{R^2} \right) \right). \end{aligned} \quad (5)$$

This expression can be considered an ordinary differential equation for the quantity in the spatial integral, which we define as  $S$ . Use of this definition results in

$$S + \lambda_1 \left( \frac{dS}{dt} + \dot{R} \frac{\tau_{rr}(R)}{R} \right) = \frac{4}{3} \eta_0 \left( \frac{\dot{R}}{R} + \lambda_2 \left( \frac{2\dot{R}^2 + R\ddot{R}}{R^2} \right) \right), \quad (6)$$

such that

$$S(R,t) = \int_R^\infty \frac{\tau_{rr}(r,t) dr}{r}. \quad (7)$$

Equation (6) is thus coupled to the radial equation of the bubble wall motion by an equation for the stress tensor evaluated at the bubble wall. Evaluating Eq. (2) at  $r=R(t)$  yields

$$\tau_{rr}(R) + \lambda_1 \frac{\partial \tau_{rr}(R)}{\partial t} = 4\eta_0 \left( \frac{\dot{R}}{R} + \lambda_2 \left( \frac{2\dot{R}^2 + R\ddot{R}}{R^2} \right) \right). \quad (8)$$

This expresses the problem as a set of three coupled nonlinear differential Eqs. (1), (6), and (8). Assuming a polytropic relationship for the internal gas pressure closes the problem. Though this assumption has been shown to have some physical limitations especially with respect to driven oscillations and thermal damping,<sup>1</sup> these will not be of primary concern to us in this paper given the constraints in amplitude excursion imposed by the linear viscoelastic limit.<sup>5,6</sup> However, it is important to keep in mind the limitations of this assumption in mind when interpreting some of the new results.

Starting with this formulation of the problem, we implement perturbation techniques and obtain numerical solutions. To achieve this, we first chose a nondimensionalization appropriate to a multiple scale perturbation technique.

The following nondimensional quantities are introduced to make the problem more appropriate to a perturbation analysis. Some of the choices reflect those taken from previous perturbation studies of Newtonian bubbles. In the Newtonian limit such that the non-Newtonian terms vanish, the results can be checked against those previously obtained,

$$\begin{aligned}\bar{r} &= r/R_0; \quad \bar{R} = R/R_0; \quad \bar{t} = t / R_0 \sqrt{\frac{\rho}{p_{go}}}; \\ \bar{\tau} &= \frac{\tau}{\eta_0} R_0 \sqrt{\frac{\rho}{p_{go}}}.\end{aligned}\quad (9)$$

Time is nondimensionalized by essentially the linear bubble resonance frequency. In this perturbation method, we will focus on bubble behavior near its natural, linear resonance, which turns out to be one of the most important time scales. The initial gas pressure in the bubble is denoted by  $p_{go}$ . The choice of nondimensionalization for the last term warrants a brief explanation. This choice originates from a Newtonian fluid, where  $\tau \sim \eta_0 \partial u / \partial r$ . It is reasonable for our work, which concentrates on elastic deviations from the Newtonian case.

The radial bubble dynamics equation [Eq. (1)] is given by

$$\begin{aligned}\bar{R}\ddot{\bar{R}} + \frac{3}{2}\dot{\bar{R}}^2 &= (1/\bar{R}^3\kappa) - w(1/\bar{R}) - (1-w)(1-\bar{a}\cos(\Omega\bar{t})) \\ &\quad - \frac{3}{\text{Re}} \int_R^\infty \frac{\bar{\tau}_{rr}(\bar{r}, \bar{t})}{\bar{r}},\end{aligned}\quad (10)$$

where we use a polytropic relationship for the exponent. The following nondimensional quantities are defined as

$$\begin{aligned}w &= \frac{2\hat{\sigma}}{p_{go}R_0}; \quad \Omega = R_0 \sqrt{\frac{\rho}{p_{go}}} \omega; \\ \text{Re} &= \eta_0 / (p_{go}\rho)^{1/2} R_0; \quad \bar{a} = \frac{p_a}{p_0},\end{aligned}\quad (11)$$

where the Reynolds number is denoted as Re. The quantity  $w$  represents a nondimensional Laplace pressure and  $\Omega$  the ratio of acoustic forcing frequency to the natural resonance frequency of the bubble. The equations for the stresses are

$$\bar{S} + \text{De} \left( \frac{d\bar{S}}{d\bar{t}} + \bar{R} \frac{\bar{\tau}_{rr}(\bar{R})}{\bar{R}} \right) = \frac{4}{3} \left( \frac{\dot{\bar{R}}}{\bar{R}} + \lambda \text{De} \frac{2\bar{R}^2 + \bar{R}\ddot{\bar{R}}}{\bar{R}^2} \right) \quad (12)$$

and

$$\bar{\tau}_{rr}(\bar{R}) + \text{De} \left( \frac{d\bar{\tau}_{rr}(\bar{R})}{d\bar{t}} \right) = 4 \left( \frac{\dot{\bar{R}}}{\bar{R}} + \lambda \text{De} \frac{2\bar{R}^2 + \bar{R}\ddot{\bar{R}}}{\bar{R}^2} \right), \quad (13)$$

and the nondimensional quantities such as the Deborah number (De) are expressed as follows:

$$\text{De} = \lambda_1 / R_0 \sqrt{\frac{\rho}{p_{go}}}; \quad \lambda = \frac{\lambda_2}{\lambda_1}. \quad (14)$$

The Deborah (De) number, a nondimensional number in non-Newtonian fluid dynamics, expresses the ratio of two time scales: the fluid to that of the flow.<sup>15</sup> This gives an estimate of the relative importance of elastic to viscous forces. It is usually taken as the ratio of a characteristic time of the fluid to a characteristic time for deformation. In this case, the Deborah number is defined as ratio of the relaxation time to the natural frequency of the bubble. The ratio of the retardation time to the relaxation time denoted by  $\lambda$  is expected to be a small quantity for relevant biological or polymeric fluids.<sup>5,15</sup> It should be noted again that in the limit the Deborah number goes zero, the Newtonian expressions for the viscous terms are recovered in Eqs. (10), (12) and (13).

## II. PERTURBATION ANALYSIS

Perturbation analyses have been used previously to describe the weakly nonlinear response of an acoustically forced gas bubble in a Newtonian fluid. Only methods that yield a uniform expansion for the nonlinear oscillations should be used.<sup>16</sup> Nayfeh and Saric were among the first to use the method of multiple scales to analyze a bubble in an inviscid, slightly compressible fluid governed by the Herring equation.<sup>17</sup> In a series of papers, Prosperetti used the method of averaging to examine the transient and steady-state response of a bubble governed by the Rayleigh-Plesset equation.<sup>18,19</sup> The Rayleigh-Plesset equation has been subsequently reexamined in a series of papers using the multiple scales analysis.<sup>20,21</sup> All of these studies were based on small-amplitude acoustic forcing and hence small oscillations about the equilibrium radius. We seek to undertake a similar analysis for the non-Newtonian, viscoelastic fluid. For notational convenience, we will drop the bars (denoting the nondimensional quantities) introduced in the previous section.

Following the previous approaches,<sup>18,19</sup> we seek a perturbation solution for small forcing, so we first expand the equilibrium radius in terms of relative amplitude  $x$ ,

$$R = 1 + x, \quad (15)$$

keeping terms to second order in  $x$ . We substitute Eq. (15) into Eqs. (10), (12), and (13) and obtain the following equations:

$$\begin{aligned}\ddot{x} + \omega_0^2 x &= F \cos(\Omega t) + \left( -\frac{3}{2}\dot{x}^2 + \alpha_1 x^2 - xF \cos(\Omega t) \right) \\ &\quad + \left( -\alpha_2 x^3 + x^2 F \cos(\Omega t) + \frac{3}{2}\dot{x}^2 x \right) + \alpha_3 S,\end{aligned}\quad (16)$$

$$\begin{aligned}S + \text{De} \left( \frac{dS}{dt} + \tau_{rr}(\dot{x} - x\dot{x}) \right) &= \frac{4}{3} ((\dot{x} - x\dot{x}) \\ &\quad + \lambda \text{De} (\ddot{x} + (2\dot{x}^2 - x\ddot{x}))),\end{aligned}\quad (17)$$

$$\tau_{rr} + \text{De} \frac{\partial \tau_{rr}}{\partial t} = 4 ((\dot{x} - x\dot{x}) + \lambda \text{De} ((2\dot{x}^2 - \ddot{x}x) + \ddot{x})), \quad (18)$$

where we have introduced the following quantities:



$$\alpha_1 = \frac{9}{2}(\kappa + 1) - 2w; \quad \alpha_2 = \frac{\kappa}{2}(9\kappa^2 + 18\kappa + 11) - 3w; \quad (19)$$

$$\alpha_3 = \frac{-3}{\text{Re}}; \quad F = (1 - w)\bar{a}.$$

First, we employ the method of multiple scales to obtain an analytical solution near the primary resonance such that the forcing is near the natural linear frequency for free oscillations. In nonlinear oscillations of the bubble, the amplitude and phase of the oscillations depend upon each other. A standard perturbation scheme will fail to capture the variations of the amplitude with the phase and results in a nonuniform expansion. However, these problems may be overcome by allowing the solution to be a function of independent time scales. The amplitude and phase interaction tends to occur at slower scales than natural oscillations. We approximate this frequency as  $\omega_0^2 = 3\kappa - w$ . We need to order the excitation, the nonlinearity, and the viscoelastic damping effects so that their contributions appear at the same time in the perturbation scheme.<sup>16,20,21</sup> In this case, we define with the small parameter  $\varepsilon$ ,

$$F = \varepsilon^3 f; \quad x = \varepsilon u. \quad (20)$$

The viscoelastic damping effects from the stress Eqs. (12) and (13) need to appear at the same order. Our choice will be  $1/\text{Re} \sim O(\varepsilon)$  to match with the expansions of Eqs. (17) and (18). Using Eq. (20), the radial equation (16) can be expressed as

$$\ddot{u} + \omega_0^2 u = \varepsilon^2 f \cos(\Omega t) + \varepsilon(-\frac{3}{2}\dot{u}^2 + \alpha_1 u^2 + \alpha_3 S) + \varepsilon^2(-\alpha_2 u^3 + \frac{3}{2}\dot{u}^2 u). \quad (21)$$

We can implement the method of multiple scales to obtain expansions for the dependent variables

$$u(t; \varepsilon) = u_0(T_0, T_1, T_2) + \varepsilon u_1(T_0, T_1, T_2) + \varepsilon^2 u_2(T_0, T_1, T_2) + \dots, \quad (22)$$

$$\tau_{rr}(t; \varepsilon) = \tau_0(T_0, T_1, T_2) + \varepsilon \tau_1(T_0, T_1, T_2) + \varepsilon^2 \tau_2(T_0, T_1, T_2) + \dots, \quad (23)$$

$$S(t; \varepsilon) = S_0(T_0, T_1, T_2) + \varepsilon S_1(T_0, T_1, T_2) + \varepsilon^2 S_2(T_0, T_1, T_2) + \dots, \quad (24)$$

where

$$T_n = \varepsilon^n t; \quad n = 0, 1, \dots, \quad (25)$$

and the time derivatives can be expressed in terms of the multiple time scales as

$$d/dt = \sum_{n=0} \varepsilon^n D_n, \quad D_n = \partial/\partial T_n, \quad (26a)$$

$$d/dt = D_0 + \varepsilon D_1 + \varepsilon^2 D_2 + \dots, \quad (26b)$$

$$d^2/dt^2 = D_0^2 + 2\varepsilon D_0 D_1 + \varepsilon^2(D_1^2 + 2D_0 D_2) + \dots$$

Substituting Eqs. (22)–(24), and (26) into Eqs. (16)–(18), and equating powers of epsilon, we obtain

$$D_0^2 u_0 + \omega_0^2 u_0 = 0 \quad O(\varepsilon^0), \quad (27)$$

$$S_0 + \text{De}(D_0 S_0) = 0, \quad (28)$$

$$\tau_0 + \text{De}(D_0 \tau_0) = 0. \quad (29)$$

We see from Eqs. (28) and (29) that, to first order, the equations for the stresses decouple such that in this case we need only consider the  $S$  equations, the integral of the stress, in order to include the damping effects. We need to have the damping effects come in at the same time as the forcing, so we set these variables to zero in Eqs. (28) and (29),

$$S_0 = 0; \quad \tau_0 = 0. \quad (30)$$

The next order equations can be expressed as

$$D_0^2 u_1 + \omega_0^2 u_1 = -2D_0 D_1 u_0 - \frac{3}{2}(D_0 u_0)^2 + \alpha_1 u_0^2 O(\varepsilon^1), \quad (31)$$

$$S_1 + \text{De}(D_0 S_1) = \frac{4}{3}(D_0 u_0 + \lambda \text{De}(D_0^2 u_0)), \quad (32)$$

and performing the expansion out to second order in epsilon yields

$$D_0^2 u_2 + \omega_0^2 u_2 = -D_1^2 u_0 - 2D_0 D_1 u_1 - 2D_0 D_2 u_0 - 3(D_0 u_0)(D_0 u_1) + 2\alpha_1 u_0 u_1 - \alpha_2 u_0^3 + \frac{3}{2}u_0(D_0 u_0)^2 - 3(D_0 u_0)(D_1 u_0) + \alpha_3 S_1 + f \cos[(\omega_0 T_0 + \sigma T_2)] O(\varepsilon^2) \quad (33)$$

$$\Omega = \omega_0 + \varepsilon^2 \sigma,$$

where  $\sigma$  represents the detuning parameter (frequency of the excitation).<sup>16</sup> The solution to Eq. (33) can be expressed as

$$u_0 = A(T_1, T_2) \exp(i\omega_0 T_0) + c.c. \quad (34)$$

*c.c.*—complex conjugate

for the unknown complex function  $A$ . Substituting this into Eq. (31) yields

$$D_0^2 u_1 + \omega_0^2 u_1 = -2i\omega_0 D_1 A e^{i\omega_0 T_0} - \frac{3}{2}\omega_0^2 (A\bar{A} - A^2 e^{i2\omega_0 T_0}) + \alpha_1 (A^2 e^{i2\omega_0 T_0} + A\bar{A}) + c.c., \quad (35)$$

where the “ $\sim$ ” symbol denotes the complex conjugate. Using the freedom of multiple scales to eliminate the secular terms (those not uniformly valid as time increases), we let

$$A = A(T_2), \quad (36)$$

so that the first term on the left-hand side goes to zero and we can solve Eq. (35),

$$u_1 = c_1 A^2 \exp(2i\omega_0 T_0) + c_2 A\bar{A} + c.c., \quad (37)$$

$$c_1 = -\frac{\alpha_1 + \frac{3}{2}\omega_0^2}{3\omega_0^2}; \quad c_2 = \frac{\alpha_1 - \frac{3}{2}\omega_0^2}{\omega_0^2}.$$

Likewise, we substitute Eq. (37) into the equation for  $S$ , Eq. (32). We assume a solution of the form

$$S_1 = C \exp(i\omega_0 T_0) + ED + c.c. \quad (38)$$

The term  $ED$  depends on the initial conditions and is exponentially decaying. One objective of this analysis is to examine steady-state responses where this term does not contrib-

ute. In this case, we set it equal to zero and solve for the constant

$$C = \frac{4}{3} \frac{i\omega_0 - \text{De} \lambda \omega_0^2}{1 + i\text{De} \omega_0}, \quad (39)$$

which can be separated into its real and imaginary parts,

$$C = c_r + ic_i, \quad (40)$$

$$c_r = -\frac{4}{3} \frac{\text{De} \omega_0^2 (\lambda - 1)}{(1 + \text{De}^2 \omega_0^2)}, \quad (41)$$

$$c_i = \frac{4}{3} \frac{\omega_0 (1 + \text{De}^2 \lambda \omega_0^2)}{(1 + \text{De}^2 \omega_0^2)}. \quad (42)$$

It is advantageous to do this separation because the amplitude and phase equations will be separated into real and imaginary parts in the method of multiple scales, and these coefficients [Eqs. (41), (42)] have some physical significance. The imaginary part Eq. (42) corresponds to the storage or elastic component in the fluid and the real part Eq. (41) is proportional to the viscous damping or loss due to dissipation. A Newtonian fluid will only have a viscous loss term proportional to its natural frequency, as seen by taking the limit as the Deborah number goes to zero. As the ratio of the retardation to relaxation time ( $\lambda$ ) approaches one, the magnitude of the storage coefficient decreases for increasing loss coefficient.

We can substitute the results of Eqs. (34), (37), and (38) into Eq. (33), resulting in

$$\begin{aligned} D_0^2 u_2 + \omega_0^2 u_2 = & (-2i\omega_0 A' + c_4 A^2 \tilde{A} + \frac{1}{2} f \exp(i\sigma T_0) \\ & + \alpha_3 (c_r + ic_i) A) e^{i\omega_0 T_0} + \text{nst} + c.c., \\ c_4 = & \frac{20\alpha_1^2 - 30\alpha_1 \omega_0^2 - 18\alpha_2 \omega_0^2 + 27\omega_0^2}{6\omega_0^2}, \end{aligned} \quad (43)$$

where the prime denotes a derivative with respect to  $T_2$  and “nst” refers to nonsecular terms. We can set the secular term in Eq. (43) to zero and separate into real and imaginary parts by introducing

$$A = \frac{1}{2} a(T_2) \exp(i\beta(T_2)). \quad (44)$$

The real and imaginary parts are

$$a\beta' + \frac{c_4}{8} a^3 + \frac{f}{2} \cos \gamma + \frac{a}{2} \alpha_3 c_r = 0, \quad (45)$$

$$-a' \omega_0 + \frac{f}{2} \sin \gamma + \frac{a}{2} \alpha_3 c_i = 0, \quad (46)$$

respectively. Eliminating  $\beta$  yields the following equations:

$$a\sigma\omega_0 - a'\gamma' \omega_0 + \frac{c_4}{8} a^3 + \frac{f}{2} \cos \gamma + \frac{a}{2} \alpha_3 c_r = 0, \quad (47)$$

$$-a' \omega_0 + \frac{f}{2} \sin \gamma + \frac{a}{2} \alpha_3 c_i = 0, \quad (48)$$

$$\gamma = \sigma T_2 - \beta. \quad (49)$$

The steady-state response, corresponding to the stationary solutions to Eqs. (47) and (48), is

$$a\sigma = -\frac{c_4}{8\omega_0} a^3 - \frac{f \cos \gamma}{2\omega_0} - \frac{a}{2\omega_0} \alpha_3 c_r, \quad (50)$$

$$\frac{f}{2} \sin \gamma = -\frac{a}{2} \alpha_3 c_i. \quad (51)$$

These equations can be combined into a single equation that describes analytically the frequency-dependent amplitude response of the bubble,

$$f^2 = a^2 (\alpha_3 c_i)^2 + a^2 \left( 2\sigma\omega_0 + \frac{c_4}{4} a^2 + \alpha_3 c_r \right)^2. \quad (52)$$

This equation can be solved numerically to obtain a frequency response curve (amplitude,  $a$ , versus the frequency detuning,  $\sigma$ ). The response for different Deborah numbers indicates the effect of elasticity on the primary resonance. Some of these results are shown in Figs. 1 and 2. The results shown in Fig. 1. are the same case except at Deborah numbers of 0.0, 1.0, and 2.0 for fixed value of retardation to relaxation time. The  $\text{De}=0.0$  case corresponds to the Newtonian response. We notice for increasing Deborah number, and hence increasing elastic properties in the fluid, the amplitude of response becomes greater. The bubble does not exhibit nonlinear softening effects in the Newtonian ( $\text{De}=0.0$ ) case. However, these effects become apparent for Deborah numbers of 1.0 and 2.0. In these cases, the amplitude jumps to a lower value for decreasing frequency and a higher one for increasing frequency. Bubbles in Newtonian fluids also exhibit this softening phenomenon,<sup>17,18,20</sup> but this effect appears at lower forcing amplitude with the inclusion of viscoelasticity. A possible physical explanation for this is that the addition of elasticity seems to cause the bubble to stay at its point of maximum expansion longer. It appears it takes longer with elasticity for the stresses in the fluid to begin initiating the bubble collapse process.

Figure 2 shows the frequency response curve for  $\text{De}=1.0$  and for values of the ratio of the retardation to relaxation time of 0.0, 0.1, and 0.2. The linear Maxwell model corresponds to the  $\text{De}=0.0$  case. The softening effect diminishes with increasing retardation time. A possible explanation for this result might be that extra dissipation associated with the Jeffreys model damps out the nonlinearity even at these low amplitudes of forcing. The retardation term for this approximation can be seen as a loss that is proportional to the acceleration of the bubble wall.

The stability of these response curves for steady-state motion can be investigated by linearizing the amplitude and phase equations about the singular points. Information is gained about the local stability by examining small disturbances or perturbations about these points,

$$a = a_0 + a_1, \quad \gamma = \gamma_0 + \gamma_1. \quad (53)$$

The zero subscript denotes the singular points and the one subscript the disturbances about them. The eigenvalues of the coefficient matrix of the linearized equation determine the stability characteristic.<sup>16</sup> The system is stable if the characteristic roots have negative real parts.<sup>16</sup> This method was employed to investigate the stability of Eqs. (50) and (51). The structural characteristics that were examined appear

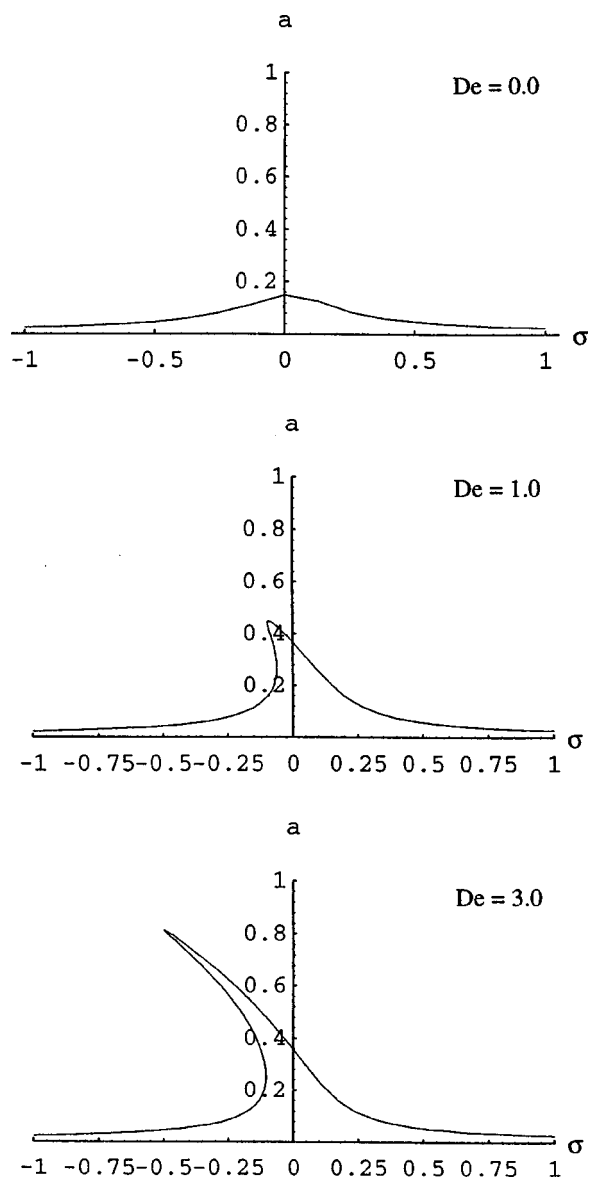


FIG. 1. Shown (from top to bottom) are the nondimensional frequency response curves for  $De=0.0$ ,  $1.0$ , and  $3.0$ . The other parameter values are  $\kappa=1.4$ ,  $w=0.145$ ,  $1/Re=0.1$  and  $\lambda=0.1$ . Note that the nonlinear softening response is visible for the viscoelastic cases but not the Newtonian case ( $De=0.0$ ). Moreover, this nonlinearity increases with increasing Deborah number.

quite similar to the Newtonian results. The stability requirements for steady-state motion are shifted by an overall constant proportional to the real and imaginary damping coefficients. We might expect more interesting results if we retained higher order terms from the constitutive equation expansions.

Numerical and experimental studies have shown the occurrence of secondary harmonics, namely superharmonics and subharmonics from acoustically driven Newtonian bubbles.<sup>1,2</sup> The method of multiple scales has been used to analytically examine these responses. Nayfeh and Saric's initial study determined the superharmonic responses and pressure amplitude threshold for the first subharmonic resonance from a form of the Herring equation.<sup>16</sup> Nayfeh and Mook used this same ordering of the damping, nonlinearity, and excitation terms in the perturbation analysis for a study of a

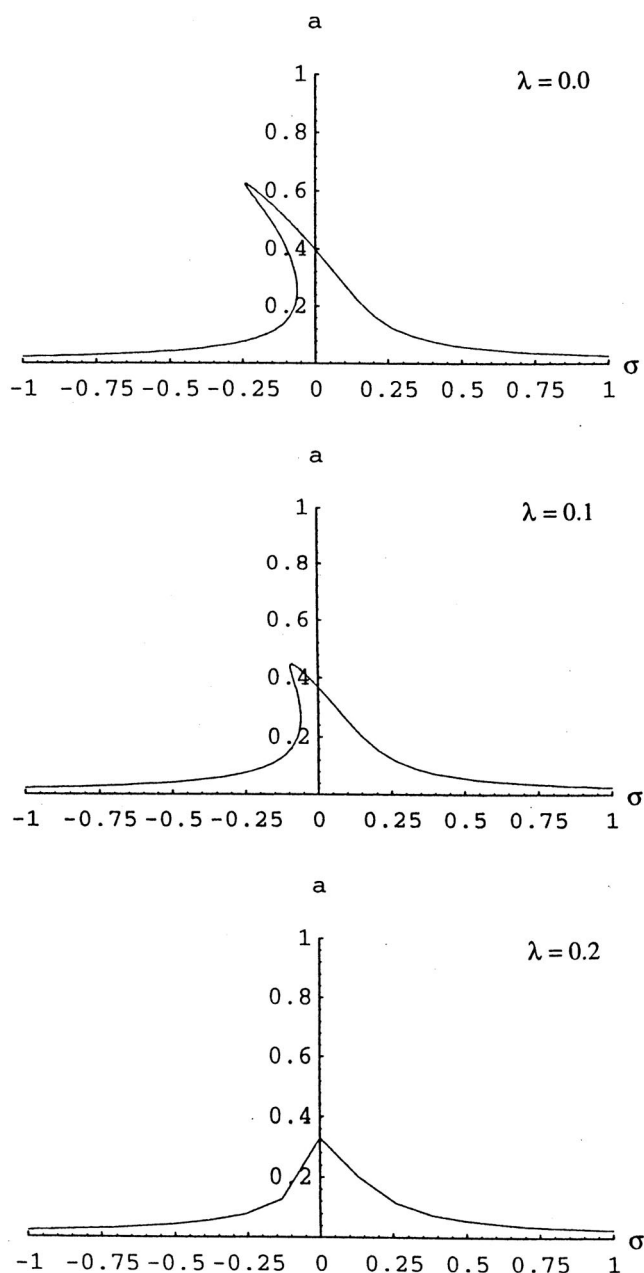


FIG. 2. Increases in the retardation time of the fluid damp of the frequency response curves, shown here for  $De=1.0$  (other parameters are the same as in Fig. 1) and  $\lambda=0.0$ ,  $0.1$ , and  $0.2$  (shown top to bottom). This indicates that a bubble response in a linear Jeffreys fluid will be diminished compared to that in a linear Maxwell fluid.

related nonlinear oscillation problem.<sup>15</sup> Francescutto and Nabergoj followed this ordering approach in their studies of the first subharmonic in the Rayleigh-Plesset equation.<sup>16,17</sup> However, in a subsequent paper Nayfeh addressed the limitations and validity of this ordering and offered a uniformly valid alternative.<sup>22</sup> In particular, he demonstrated that the previously used ordering is not valid for large times due to the fact that resonant terms are produced by the quadratic terms in the equation before a self-interaction by the nonlinearity. Using the alternative ordering, Nayfeh found a region where the subharmonics may be excited (depending on the initial conditions) which was not revealed in the previous studies.<sup>22</sup> In the improved first subharmonic ordering, Nay-



feh examines both the cases of small damping for closely tuned oscillations and larger damping for a case that is not as closely tuned.<sup>22</sup> The closely tuned subharmonic case refers to a nearness of  $\Omega$  to  $2\omega_0$  and the detuning  $\sigma$  can be defined as

$$\Omega = 2\omega_0 + \varepsilon^2\sigma. \quad (54)$$

The additional viscoelastic equations can be easily extended to Nayfeh's closely tuned case using the same expansions (23) and (34) and results in Eq. (30) for the primary harmonic where damping is scaled so it appears in the second order equations of the expansions. To first order, we expect the effects similar to those on the primary resonance from the real and imaginary constants. (We will leave a comprehensive study of the secondary harmonics, in particular the subharmonic case, for numerical studies that follow.) The reason for this being that a numerical solution of the system preserves more of the physics of the constitutive equations.

### III. NUMERICAL ANALYSIS

In this section, we obtain numerical solutions to Eqs. (1), (6) and (8). For these studies, we adopt a change in the choice of nondimensionalization of several quantities. The choice of Deborah number used in Eq. (14) was appropriate for investigating forcing near the natural linear frequency of the bubble. In that case, the results may easily be checked against previous perturbation solutions in Newtonian limit. In these numerical investigations of the complete set of equations, it is more desirable that the nondimensional numbers reflect the way the inertial and elastic forces depend on the forcing frequency. In this section, the Deborah and Reynolds numbers are rescaled to reflect the acoustic forcing frequency for off-resonance cases. Time is re-dimensionalized such that

$$\bar{t} = \omega t, \quad (55)$$

then the Deborah number is rewritten as

$$\text{De} = \lambda_1 \omega, \quad (56)$$

and also the Reynolds number is rewritten,

$$\text{Re} = \rho \omega R_0^2 / \eta_0. \quad (57)$$

This definition of the Deborah number approximates Eq. (14) as the acoustic forcing approaches the linear resonance frequency. Also with this choice, a Deborah number of order one or greater represents physically reasonable quantities for studies of polymeric and biological fluids. A nondimensional rescaling of the stress tensor was examined; however, it was found that it was still physically and numerically reasonable to essentially retain the previous nondimensionalization of the stress tensor with the substitution of the ambient pressure for the equilibrium bubble pressure.

First, we consider a case of acoustic forcing away from the bubble's natural frequency. We examine a 0.5-micron equilibrium radius bubble at 1.0 MHz forcing for various values of Reynolds and Deborah numbers. In light of potential biomedical applications related to this work, the values are chosen to roughly approximate biological fluids or tissue.<sup>5</sup> Polymer stabilized (xanthan gum) bubble clouds have been manufactured for underwater acoustics applications<sup>25</sup> with Deborah and Reynolds numbers compa-

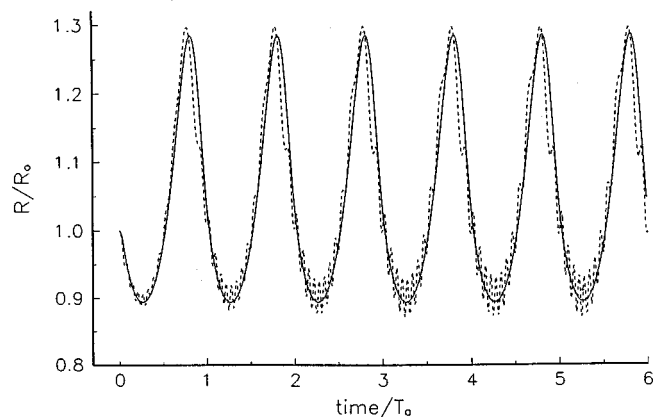


FIG. 3. The oscillatory behavior of a 0.5-micron radius bubble (0.2 MPa, 1.0 MHz,  $\text{Re}=0.2$ ) demonstrates the differences in bubble response in a viscoelastic linear Maxwell fluid at  $\text{De}=1.0$  (dashed line) and a Newtonian fluid (solid line). A slight phase shift exists between the two cases. Small oscillations occur near the cycle minima for the viscoelastic case.  $T_a$  is the acoustic period.

table to those used in generating Figs. 9–12. The pressure amplitudes are kept low (usually below 0.2 MPa) in order to stay within the restrictions of linear viscoelasticity. The surface tension is kept fixed so the effects of varying  $\text{Re}$  and  $\text{De}$  number can be discerned. For all the numerical cases, the interior gas is assumed to be air, such that  $\kappa=1.4$ , and that the fluid has surface tension ( $72.5 \text{ dyn/cm}^2$ ) and density ( $0.999 \text{ cm}^3/\text{gm}^3$ ) of that of water. Actual values for biological fluids and tissue are probably different; however, such values are not well established and the aim of this initial paper is to examine the effects of viscoelasticity. In the limit that the Deborah number, elasticity of the fluid, goes to zero a viscous Newtonian fluid is recovered ( $\lambda_1=0$ , Newtonian fluid). Figure 3 shows bubble oscillations where the  $\text{De}=1.0$  and  $\text{Re}=0.2$  compared to a Newtonian fluid of the same Reynolds number.

Several novel features distinguish the viscoelastic case from the corresponding Newtonian case. First, the overall phase of the oscillation is slightly shifted from the Newtonian case. This may be due to the presence of elasticity, which results in the storage of energy in the fluid. Furthermore, the viscoelastic bubble reaches a maximum slightly before the Newtonian bubble. Near the cycle minimum there are many small-scale oscillations, essentially manifestations of relatively small fluctuations in radius. One initial concern might be that these oscillations are numerical artifacts and not physical in origin. However, numerical tests varying the accuracy parameters in the integration method were done to check for these problems; robustness was verified. The oscillations were also found to be a function of the physical parameters in the study, thus casting further doubt on the notion that these oscillations are due to numerical effects. Finally, it should be noted that researchers who have examined viscoelastic bubble oscillations previously and related viscoelastic flow problems have encountered similar oscillatory phenomena, which they concluded to be physical in nature.<sup>23</sup> Our conclusion is that these oscillations are probably due to weak coupling of the elastic fluid effects with the bubble's motion. They occur near the oscillation cycle mini-

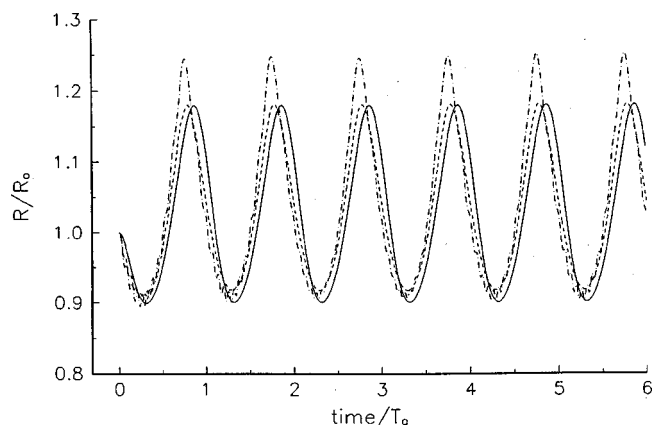


FIG. 4. The 0.2-micron bubble from Fig. 3 is shown for  $Re=0.05$  in Newtonian (solid line),  $De=1.0$  (dashed line) and  $De=3.0$  (dot-dash line) fluids. The lower Reynolds number leads to a damping of the small oscillations, though the phase shift effect remains visible. The amplitude of radial excursion increases with increasing Deborah number, a result that is consistent with the perturbation analysis.

num as the bubble wall velocity begins to slow down, consistent with our previous notions that time is required for the stress effects to catch up to bubble's wall motion.

We further demonstrate that these small-scale oscillations are a function of the physical parameter, as indicated in Fig. 4; the Reynolds and Deborah are set to  $Re=0.05$  and  $De=1.0, 3.0$ ; the Newtonian case ( $De=0.0$ ). The smaller Reynolds number corresponds to an increased viscosity damping. The small oscillations near the cycle minima have been diminished and the overall phase shift from the Newtonian case seen previously remains visible. In this case, an increase from  $De=0.0$  to  $De=1.0$  results in a visible phase shift but little change in amplitude. Increasing the Deborah number from 1.0 to 3.0 results in clear growth in the amplitude of the response. For these parameters it appears a sufficient Deborah number must be reached for the amplitude effect to develop.

A plot of the radial stress tensor at the bubble wall for the  $De=1.0$  and  $De=3.0$  cases from Fig. 4 is given in Fig. 5. For  $De=3.0$ , the plot shows some stress oscillations corresponding with small oscillations in radius. The excursions in stress are less in the  $De=1.0$  case compared to the  $De=3.0$  condition. A plot of the bubble wall velocity further illus-

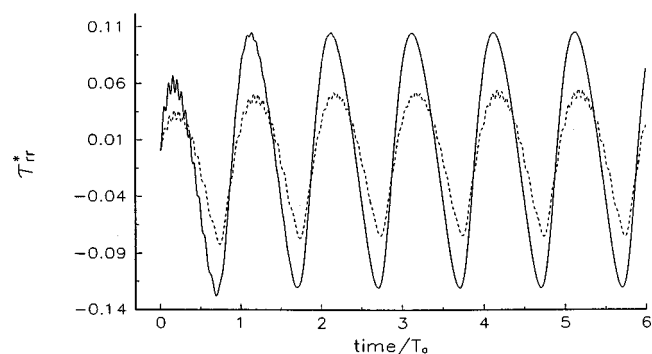


FIG. 5. The radial stress tensor at the bubble wall for the same parameters given in Fig. 4 is shown for  $De=1.0$  (solid line) and  $De=3.0$  (dashed line) cases. The elasticity seems to influence the magnitude of the stress produced at the bubble wall.

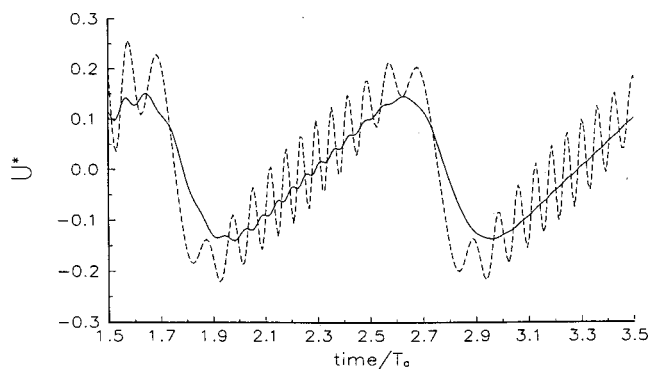


FIG. 6. The bubble wall velocity for the  $De=3.0$  (dashed line) and  $De=1.0$  (solid line) cases from Fig. 5. A steep drop in velocity followed by fluctuations corresponds with a less intense collapse.

trates this point (see Fig. 6). During the initial moments of collapse, the greater Deborah number results in a faster collapse. As the velocity begins to bottom out, the elastic stress starts inducing oscillations in the radius and the radial velocity. These effects serve to lessen the magnitude of the overall collapse strength. This phenomenon is a direct consequence of stress relaxation effects incorporated in the linear Maxwell model. Furthermore, these results hold important implications in the assessment of cavitation damage in media with increasing elasticity. Kim, using a more complicated objective model, made some similar observations for free bubble oscillations.<sup>13</sup> Some of the available experimental evidence indicates that polymeric additives may suppress damage effects resulting from bubble collapse, at least in the hydrodynamic case.<sup>24</sup> Our results offer physical insight into the possible governing mechanisms behind this important effect.

The previously depicted results are probably due to a weak coupling between the elastic properties of the fluid and the bubble oscillations. More profound effects are exhibited for near-resonance forcing when compared with the Newtonian case. This is shown in Fig. 7. The secondary resonance shown in the dashed curve is not present in the corresponding Newtonian case. Hence, an additional resonance effect associated with the elasticity of the fluid is manifest. While

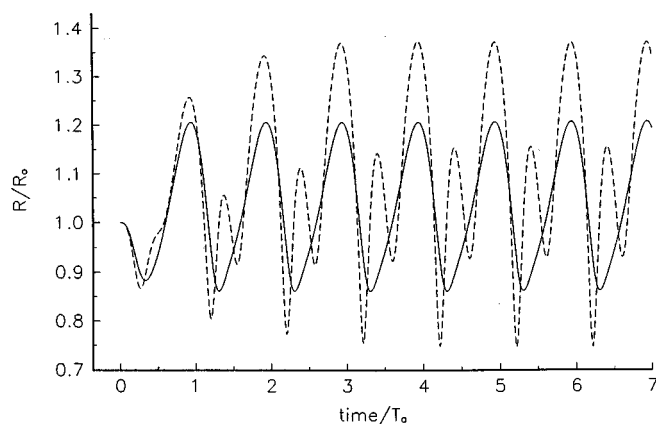


FIG. 7. A bubble's harmonic response appears to be linked to the fluid's viscoelastic properties under certain conditions. A 0.5-micron radius bubble forced near resonance (6.4 MHz, 0.2 MPa,  $Re=1.93$ ) in a  $De=1.0$  (dashed line) fluid reveals a secondary harmonic. The corresponding Newtonian case has the expected single harmonic component.

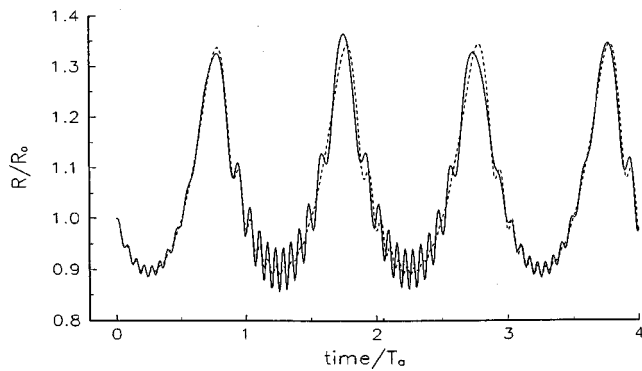


FIG. 8. The linear Jeffreys model (dashed line) for  $\lambda=0.1$  for a 0.5-micron radius bubble ( $Re=0.3$ ,  $De=2.0$ ) exhibits damped small oscillations when compared with the corresponding Maxwell fluid (solid line) case for the same parameters. These results agree qualitatively with the perturbation results.

only heightened amplitude effects were seen in the perturbation analysis, the inclusion of the complete stress equations serves to uncover an additional secondary resonance. The previously considered off-resonance case shows subtle minor variation from the Newtonian case, but here we see a more dramatic difference. In particular, this result has important implications for contrast agent harmonic imaging applications. It indicates that the occurrence of secondary resonances may be a function of specific tissue properties. Modeling tissue as viscous Newtonian fluid may not be an appropriate assumption for the prediction of secondary harmonics in sufficiently elastic tissue. Likewise, at relatively lower amplitudes of acoustic forcing, tissue elasticity may enhance secondary harmonic growth despite the highly viscous nature of the medium. Also, it should be noted a greater maximum radius is reached with the addition of elasticity. This is an important parameter for accessing potential inertia cavitation effects. The role maximum radius value plays is key in the development of the ultrasound cavitation safety criteria known as the Mechanical Index (MI).<sup>4,8</sup> This implies that tissue elasticity may need to be incorporated in future formulations of the MI.

In the perturbation scheme, the inclusion of the retardation time with the Jeffreys model results in an increasing damping of the amplitude response. This result agrees qualitatively with Shima and Tomita's study of viscoelastic bubble oscillations with the three-constant Oldroyd model.<sup>14</sup> In Fig. 8, we show that the Jeffreys model damps out oscillations that are present in the linear Maxwell model for the same set of parameters. Additional numerical studies indicate that increasing the ratio of retardation to relaxation times further damps the oscillations. We leave a more comprehensive examination of the retardation term to future studies.

As mentioned above, subharmonic responses have been observed theoretically and experimentally for bubbles in Newtonian fluids. This effect, however, has not been thoroughly investigated for viscoelastic bubbles. We will examine the 2/1 subharmonic for a 0.1-mm radius bubble driven at roughly twice its natural frequency, 64.74 kHz for a 0.04 MPa pressure amplitude using the linear Maxwell model. These parameters are chosen because subharmonic behavior

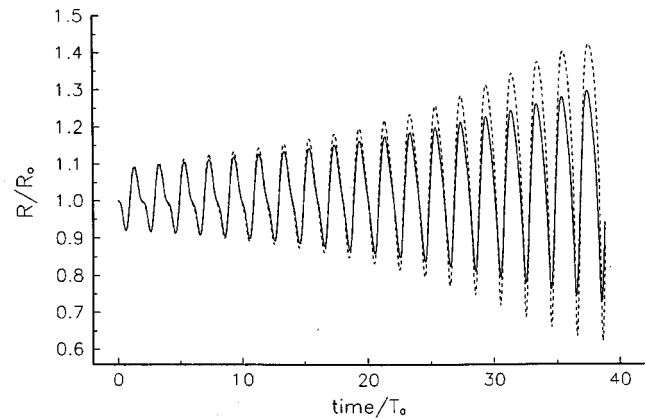


FIG. 9. The subharmonic response (0.1 mm radius, 64.74 kHz, 0.04 MPa,  $Re=203$ ) at  $De=1.0$  (dashed line) shows a more rapid growth when compared with the corresponding Newtonian ( $De=0.0$ ) (solid line) case. Notice the heightened amplitude grows for a longer forcing period.

in kHz bubbles is attainable at much lower pressure amplitudes than for micron-size bubbles at megahertz frequencies. Figure 9 shows the case where  $Re=203$  (20 cP) for a viscous Newtonian fluid, and for a viscoelastic fluid where  $De=1.0$ . The higher Reynolds number in this case in part reflects the larger equilibrium bubble radius. For Reynolds numbers smaller than this value it was found that the subharmonic structure was obscured due to viscous damping. We notice a faster growth in the radial response for the  $De=1.0$  case as compared to the corresponding Newtonian case. Indeed, the chosen parameter values allow for sufficient dissipation to permit observation of elastic effects and also restrict the amplitude excursions to be within the linear viscoelastic deformation limits. For the same Reynolds number, the Newtonian case is plotted against the  $De=3.0$  fluid in Fig. 10. This elevation in elasticity yields an even greater increase in the amplitude of the radial motion; however, the oscillation amplitude reaches a maximum and appears to fall off after about 40 cycles of acoustic forcing. We believe that the growth and decay is due at least in part to the elastic component of the fluid. However, our results must be viewed in light of our omission of thermal damping, which becomes more important in the parameter range for this case. Thermal damping

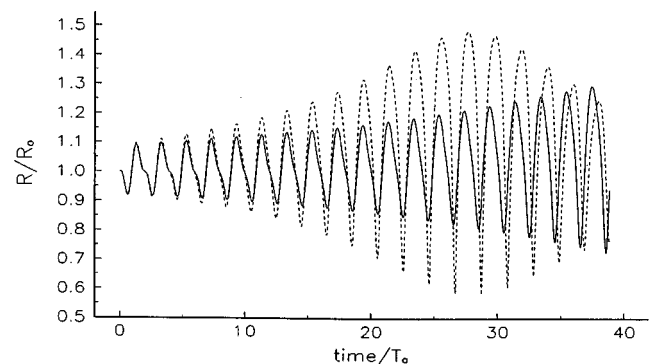


FIG. 10. A rapid growth of bubble oscillations occurs for  $De=3.0$  fluid (dashed line) when compared with the Newtonian case ( $De=0.0$ ). The subharmonic for  $De=3.0$  reaches a maximum during the first 40 cycles of forcing (compare with the  $De=1.0$  case in Fig. 9).

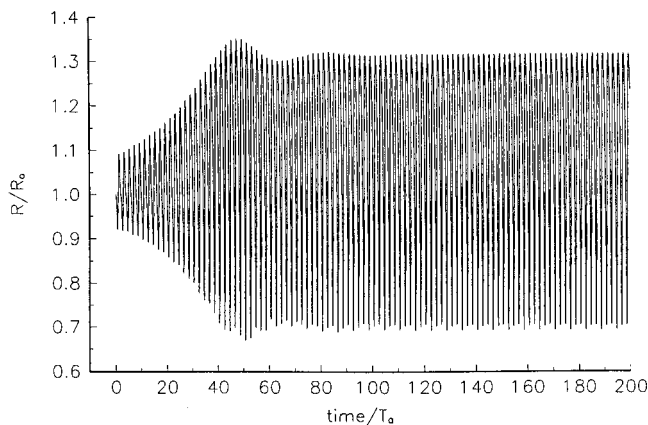


FIG. 11. A bubble in a Newtonian fluid ( $De=0.0$ ) forced by the given subharmonic excitation (see the caption for Fig. 9) reaches a steady-state excursion amplitude after about 55 cycles of forcing.

may in fact reduce the pronounced differences seen here between the viscous and viscoelastic cases.

The Newtonian case was examined over upward of 100 cycles of forcing, as shown in Fig. 11. After about 45 cycles, the subharmonic reaches a maximum and it subsequently decreases over the next 10 cycles to a steady-state value. The non-Newtonian cases for various Deborah numbers were also examined over long periods of forcing. Particularly dramatic effects appeared for  $De=10.0$ , as shown in Fig. 12. The subharmonic not only reaches maximum much more rapidly than in the Newtonian case, but its amplitude undergoes a beat-type modulation. For lower Deborah numbers, we see the gradual onset of separate amplitude packets, but eventually these effects would give way to the steady-state subharmonics observed in the Newtonian case. However, at  $De=10$  we see a full modulation effect over many cycles of forcing. The motion is itself a periodic subharmonic but appears to be modulated in a periodic fashion.

It is important to note the two simultaneous physical interactions occurring. One is the growth of the steady-state subharmonic governed by a coupling of the free oscillations of the bubble with the acoustic forcing frequency. This is immediately present in the Newtonian case and such motion

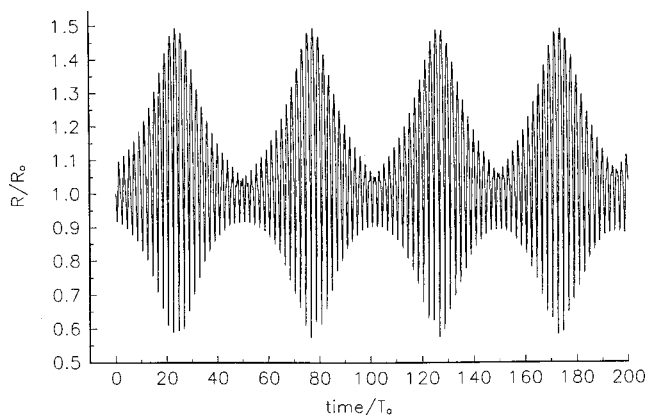


FIG. 12. For a bubble in a highly elastic fluid ( $De=10.0$ ) forced by the given subharmonic excitation (Figs. 9–11), the amplitude undergoes a novel beat modulation. Discrete groups of oscillations occur in contrast to the Newtonian case shown in Fig. 11. The width of each of these modules is related to the characteristic relaxation time of the fluid.

eventually dominates for fluids with Deborah numbers approximately less than ten. The other physical process is the addition of elasticity to the fluid, which seems to increase the oscillatory nature of the bubble response. The elasticity effects are apparently sufficient at about  $De=10.0$  that an additional, previously unknown, coupling occurs. The relaxation time of the fluid couples with the subharmonic such that it influences the magnitude of its amplitude. The characteristic time scale for amplitude modulation is on the order of the relaxation time of the fluid. The fact that the modulation time scales with the relaxation time indicates that this phenomenon is directly linked to the viscoelastic nature of the fluid. As mentioned earlier, thermal damping may modify the extent of this modulation and is the subject of further study. Nevertheless, this result is a bubble dynamics phenomenon that is unique to viscoelastic fluids and is a model prediction that lends itself to direct experimental verification.

#### IV. CONCLUSIONS

This study reveals several new and interesting features about gas bubble oscillations in viscoelastic fluids. A system of coupled nonlinear ordinary differential equations has been derived which describes the radial bubble dynamics. This formulation greatly facilitates numerical and analytical analysis of the problem. A perturbation approach using multiple scales predicts increasing damping with increasing retardation time and heightened amplitude response for increasing Deborah number. The additional elasticity adds a further softening of the nonlinear bubble response.

While the perturbation approach includes the viscoelastic effects to first order, the numerical studies incorporate the entire constitutive equation. A slight phase shift and additional oscillations distinguish the linear Maxwell case from the Newtonian case. The addition of a retardation term within the Jeffreys model damps the oscillations, a result also predicted by the perturbation theory. Finally, the addition of elasticity to the fluid produces some novel effects in the study of subharmonic excitations for kHz forcing frequencies. While the corresponding Newtonian case reaches steady amplitude subharmonic response, the amplitude of the highly viscoelastic case may be modulated in a manner seemingly governed by the relaxation time of the fluid. The impact of thermal damping on these results will be examined elsewhere.

This work has implications for many scientific and engineering applications. It was demonstrated that a bubble's response to acoustic forcing in a viscoelastic fluid might be dramatically different than that in Newtonian fluid. The amplitude restrictions imposed by the linear viscoelastic assumptions do not allow for investigations at the high-pressure amplitudes linked to potential ultrasound bioeffects.<sup>8</sup> However, our results indicate that viscoelasticity is an important effect that warrants further investigation in the development of future medical ultrasound safety criteria. For certain conditions, an enhanced maximum radius and expansion ratio (maximum to minimum radius) is observed. The fact that this parameter depends directly on elasticity suggests the Mechanical Index criteria for medical ultra-



sound bioeffects assessment should eventually be reformulated to account for different tissue elasticity values and the contribution of the ultrasound pulse duration. Finally, for ultrasound contrast agent applications involving harmonic imaging, a Newtonian fluid model may not always be the best predictor of secondary harmonic responses.

The present formulation could be readily extended for application studies where the role of large bubble deformation is not particularly critical to the analysis. Such an application might be the scattering of acoustic waves off of polymeric-gel bubble clouds. These polymeric gels, seeded with gas bubbles, have been used as experimental models of oceanic bubble clouds in geophysical acoustic studies.<sup>25</sup> This gel model eliminates some of the experimental difficulties in investigating oceanic bubble clouds in the field. However, there is some question as to the accuracy of conventional scattering theory when applied to the resonance response of bubbles in such a viscoelastic material. A future paper by the authors will address this area of application in more detail. Another area of potential application is the study of free oscillations of bubbles in polymers formed due to pressure variations in the processing methods.<sup>26</sup>

However, many biomedical and industrial applications involve bubble deformations beyond the linear viscoelastic limit. Future work should consider the use of objective constitutive equations for the fluid.<sup>15</sup> Indeed, the present work serves as a foundation for such a study. The present formulation offers a straightforward, robust benchmark for direct comparison against such future models in the linear viscoelastic limit. Finally, it should be mentioned that future efforts should also include experimental verification of these unique viscoelastic results. Currently, little experimental work currently exists on forced or even free oscillations of bubbles in viscoelastic fluids. There is a paucity of published experimental work devoted to the forced (or even free) oscillations of bubbles in viscoelastic fluids. The contributions in this work should allow for a rigorous and direct comparison of theoretical predictions with future experimental results for linear viscoelasticity.

## ACKNOWLEDGMENTS

The authors wish to acknowledge the generous financial support of ONR, NIH and DARPA. Helpful comments and suggestions by James J. Riley, Lewis Wedgewood, and Larry Crum were greatly appreciated.

- <sup>1</sup>T.J. Leighton, *The Acoustic Bubble* (Academic, San Diego, 1994).
- <sup>2</sup>E.A. Neppiris, "Acoustic cavitation," *Phys. Rep.* **61**, 159–251 (1980).
- <sup>3</sup>W.L. Nyborg and D.L. Miller, "Biophysical implications of bubble mechanics" *Appl. Sci. Res.* **38**, 17–25 (1982).
- <sup>4</sup>R.E. Apfel and C.K. Holland, "Gauging the likelihood of cavitation from short-pulse-low-duty cycle diagnostic ultrasound," *Ultrasound Med. Biol.* **17**, 179–81 (1991).
- <sup>5</sup>Y.C. Fung, *Biomechanics: Mechanical Properties of Living Tissues* (Springer-Verlag, New York, 1981).
- <sup>6</sup>J.F. Vincent, *Structural Biomaterials*, 2nd ed. (Princeton University Press, Princeton, NJ, 1990).
- <sup>7</sup>J. Ophir and K.J. Parker, "Contrast agents in diagnostic ultrasound," *Ultrasound Med. Biol.* **15**, 319–33 (1989).
- <sup>8</sup>R.E. Apfel, "Possibility of microcavitation from diagnostic ultrasound," *IEEE Trans. Ultrason. Ferroelectr. Freq. Control* **33**, 139–142 (1982).
- <sup>9</sup>A. Shima, T. Tsujino, H. Nanjo, and N. Miura, "Study of nonlinear oscillations of bubbles in Powell-Eyring fluids," *J. Acoust. Soc. Am.* **77**, 1702–1709 (1985).
- <sup>10</sup>H.S. Fogler and J.D. Goddard, "Collapse of spherical cavities in viscoelastic fluids," *Phys. Fluids* **13**, 1135–1141 (1970).
- <sup>11</sup>I. Tanasawa and W.J. Yang, "Dynamics behavior of a gas bubble in viscoelastic liquids," *J. Appl. Phys.* **41**, 4526–4531 (1970).
- <sup>12</sup>R.Y. Ting, "Viscoelastic effect of polymers on single bubble dynamics," *AIChE J.* **21**, 810–813 (1975).
- <sup>13</sup>C. Kim, "Collapse of spherical bubbles in Maxwell fluids," *J. Non-Newtonian Fluid Mech.* **55**, 37–58 (1994).
- <sup>14</sup>A. Shima, T. Tsujino, and H. Nanjo, "Nonlinear oscillations of gas bubbles in viscoelastic fluids," *Ultrasonics* **24**, 142–147 (1986).
- <sup>15</sup>R.B. Bird, R.C. Armstrong, and O. Hassager, *Dynamics of Polymeric Liquids*, 2nd ed. (Wiley, New York, 1987), Vol. 1.
- <sup>16</sup>A.H. Nayfeh and D.K. Mook, *Nonlinear Oscillations* (Wiley, New York, 1979).
- <sup>17</sup>A.H. Nayfeh and W.S. Saric, "Nonlinear acoustic response of a spherical bubble," *J. Sound Vib.* **30**, 445–453 (1973).
- <sup>18</sup>A. Prosperetti, "Nonlinear oscillations of gas bubbles in liquids: Steady state solutions," *J. Acoust. Soc. Am.* **56**, 878–885 (1974).
- <sup>19</sup>A. Prosperetti, "Nonlinear oscillations of gas bubbles in liquids: Transient solutions and the connection between subharmonic signal and cavitation," *J. Acoust. Soc. Am.* **83**, 502–514 (1988).
- <sup>20</sup>A. Francescutto and R. Nabergoj, "Steady-state oscillations of gas bubbles in liquids: Explicit formulas for frequency-response curves," *J. Acoust. Soc. Am.* **73**, 457–460 (1983).
- <sup>21</sup>A. Francescutto and R. Nabergoj, "A multiscale analysis of gas bubble oscillations: Transient and steady-state-solutions," *Acustica* **56**, 12–22 (1984).
- <sup>22</sup>A.H. Nayfeh, "The response of single degree of freedom systems with quadratic and cubic nonlinearities to a subharmonic excitation," *J. Sound Vib.* **89**, 457–470 (1983).
- <sup>23</sup>R.E. Khayat and A. Garcia-Rejo, "Uniaxial and biaxial unsteady inflations of viscoelastic material," *J. Non-Newtonian Fluid Mech.* **43**, 31–59 (1992).
- <sup>24</sup>C. Brennen, "Some cavitation experiments in dilute polymer solutions," *J. Fluid Mech.* **44**, 51–63 (1970).
- <sup>25</sup>P.A. Hwang, R.A. Roy, and L.A. Crum, "Artificial bubble cloud targets for under-water acoustic remote sensing," *J. Atmos. Ocean. Technol.* **12**, 1289–1302 (1995).
- <sup>26</sup>H.J. Yoo and C.D. Ha, "Oscillatory behavior of a gas bubble growing or collapsing in viscoelastic liquids," *AIChE J.* **28**, 1002–1009 (1982).